Cerebral Cortex Advance Access published March 28, 2004

Brain Anatomy in Turner Syndrome: Evidence for Impaired Social and Spatial–Numerical Networks

N. Molko[1], A. Cachia[2,3], D. Riviere[1,2], J.F. Mangin[2], M. Bruandet[1], D. LeBihan[2], L. Cohen[1,4] and S. Dehaene[1]

[1]INSERM U 562, Service Hospitalier Frédéric Joliot, CEA/DSV, IFR 49, Orsay, France, [2]Unité de Neuro-Activation Fonctionnelle, Service Hospitalier Frédéric Joliot, CEA/DSV, IFR 49, Orsay, France, [3]INSERM ERM 0205, IFR 49, Service Hospitalier Frédéric Joliot, CEA/DSV, IFR 49, Orsay, France and [4]Service de Neurologie 1, Hôpital Pitié-Salpétrière, Paris, France

Analysis of brain structure in Turner syndrome (TS) provides the opportunity to identify the consequences of the loss of one X chromosome on brain anatomy and to characterize the neural bases underlying the specific cognitive profile of TS subjects which includes deficits in spatial–numerical processing and social cognition. Fourteen subjects with TS and fourteen controls were investigated using voxel-based analysis of high resolution anatomical and diffusion tensor images and using sulcal morphometry. The analysis of anatomical images provided evidence for macroscopical changes in cortical regions involved in social cognition such as the left superior temporal sulcus and orbito-frontal cortex and in a region involved in spatial and numerical cognition such as the right intraparietal sulcus. Diffusion tensor images showed a displacement of the grey–white matter interface of the left and right superior temporal sulcus and revealed bilateral microstuctural anomalies in the temporal white matter. The analysis of fiber orientation suggests specific alterations of fiber tracts connecting posterior to anterior temporal regions. Last, sulcal morphometry confirmed the anomalies of the left and right superior temporal sulci and of the right intraparietal sulcus. Our results thus provide converging evidence of regionally specific structural changes in TS that are highly consistent with the hallmark symptoms associated with TS.

Keywords: developmental dyscalculia, diffusion tensor imaging, MRI, social cognition, sulcal morphometry, Turner syndrome, voxel-based morphometry

Introduction

Turner syndrome (TS) is a genetic condition resulting from a partial or complete absence of one of the two X chromosomes in a phenotypic female (Turner, 1938). TS occurs in approximately one in 2000 liveborn females and affects an estimated 3% of all females conceived (Saenger, 1996; Ranke and Saenger, 2001). TS is associated with a well-documented physical phenotype including a short stature, ovarian failure and abnormal pubertal development and a variety of other features (webbed neck, renal dysgenesis, cardiac malformation) (Ranke and Saenger, 2001; Saenger, 1996). In contrast to this well-documented physical phenotype, the consequences of the loss of one X chromosome on brain development and brain function are far less understood. Behavioral studies suggest that the cognitive profile of TS is characterized by a discrepancy between poor non-verbal abilities and normal to strong verbal ability, in the absence of general mental retardation (Temple and Carney, 1996; Ross *et al.*, 2000; Temple and Sherwood, 2002). While the severity of the cognitive profile in TS varies widely, some hallmark symptoms include deficits in visuo-spatial and number processing, working memory and executive function, and social cognition (Ross *et al.*, 2000). Whether the psychosocial problems associated with TS result from the numerous daily life difficulties or reflect a specific impairment is still unclear. Recent studies showed impairment of affect recognition and gaze direction monitoring in TS, suggesting that these social difficulties may originate from a genuine cognitive deficit in reading socially relevant information from subtle visual cues (Elgar *et al.*, 2002; Lawrence *et al.*, 2003).

All these converging data tentatively evoke the possible impairment of multiple neural systems distributed across distinct cerebral regions. However, no brain abnormalities are obvious on visual inspection as expected in such developmental disorders where cognitive dysfunctions are more likely related to subtle neuronal and myelination changes. Nevertheless, previous volumetric MRI studies in TS showed a bilateral decrease of grey matter volumes in the parietal lobes and in parieto-occipital regions associated with a decreased volume of the subcortical gray matter and the hippocampus on both sides (Murphy *et al.*, 1993; Reiss *et al.*, 1993, 1995; Brown *et al.*, 2002). More recently, an increased volume of amygdala and of orbito-frontal cortex have been found in TS using voxel-based morphometry (Good *et al.*, 2003). Functional neuroimaging studies using positron emission tomography (PET) in TS have found a decrease of glucose metabolism in parietal and occipital regions and in the temporal cortex and insula (Clark *et al.*, 1990; Murphy *et al.*, 1997). A putative loss of occipito-parietal connections has been advanced to explain the parietal hypometabolism (Clark *et al.*, 1990; Murphy *et al.*, 1997).

In the present paper, we used high resolution anatomical and diffusion tensor images, two different MRI techniques providing complementary multi-scale information on tissue density, microstructural organization and sulcal geometry. We first performed a whole brain analysis using statistical parametric mapping (SPM) to characterize local tissue changes (Ashburner and Friston, 2000; Good *et al.*, 2001). Sulcal morphometry in regions found abnormal in the voxel-based analysis was then investigated in two candidate regions that may underlie the cognitive impairments of TS, the intraparietal sulcus (IPS) and superior temporal sulcus (STS) (Dehaene *et al.*, 1998, 1999; Allison *et al.*, 2000). Using voxel-based morphometry, high resolution T_1-weighted images have been shown to be sensitive to subtle macroscopic changes in developmental disorders (Isaacs *et al.*, 2001; Sowell *et al.*, 2001; Watkins *et al.*, 2002) and even to correlations between brain morphology and specific cognitive abilities (Maguire *et al.*, 2000; Golestani *et al.*, 2002; Sluming *et al.*, 2002). Relative to the macroscopical information provided by T_1-weighted images, diffusion tensor imaging (DTI) is a complementary MRI technique which is sensitive to microstructural features of the cerebral tissue based on the measurement of water diffusion (Klingberg *et al.*, 2000; Rose *et al.*, 2000; Le Bihan *et al.*, 2001). Through their diffusion-driven displacements, water molecules interact

with many tissue components such as cell membranes, fibers and macromolecules, allowing DTI to provide quantitative information on tissue structure at microscopic level (typically 10–30 μm) (Le Bihan *et al.*, 2001). In particular, within cerebral white matter, the coherent orientation of axons constrains water molecules to move preferentially along the main direction of neural fibers, introducing a measurable diffusion anisotropy revealing the local orientation of fibers (Pierpaoli *et al.*, 1996; Conturo *et al.*, 1999; Poupon *et al.*, 2000). In developmental and psychiatric disorders, analysis of brain structure using DTI has been shown useful in dyslexia and schizophrenia, revealing microstructural anomalies in tissue that appears normal on conventional MRI (Klingberg *et al.*, 2000; Wolkin *et al.*, 2003).

In the present study, we report the detailed analyses from these complementary MRI methods in 14 TS subjects and 14 controls.

Materials and Methods

Subjects

Fourteen subjects with TS (mean age: 24.5 ± 6.0 years, age range: 18–36 years) were recruited from the national TS association (AGAT association) and the endocrinology department of Saint-Vincent-de Paul hospital. All had the main physical features of the TS phenotype, 10 were of the 45,X karyotype, four showed a mosaic [mosaic pattern: 45,X/46,XX for three subjects, 45,X/46,Xi(Xq) for one subject]. All but one TS subjects were taking sex steroids (oestrogen and progesterone). All TS subjects were either students or employed and lived an independent life without any social help. All but one completed their high school education. The same imaging protocol was also run on 14 control subjects matched on age, sex and laterality (mean age: 24.3 ± 3.4 years, age range: 18–29 years). The mean number of study years after high school differed significantly between TS subjects and controls (respectively, 1.5 ± 0.3 and 4.4 ± 0.75 years, $P = 0.002$). All subjects gave informed consent to participate in the study, which was approved by the regional ethical committee. Arithmetic and reading achievement were also assessed using the Warrington's graded arithmetic test and a timed reading test, as a pre-test for an fMRI study during exact and approximate calculations. Warrington's graded arithmetic test, which is a test of arithmetic computations (10 additions and 10 substraction) of increasing difficulty showed that the TS subjects were impaired in number processing [mean percentage of correct responses for TS subjects and controls: 41.1 ± 4.5% and 60.1 ± 4.2%, respectively; $t(26) = 2.85$, $P = 0.008$] (Jackson and Warrington, 1986). The timed reading test of 10 words and 10 pseudo-words showed that, although TS subjects were slower in reading both types of stimuli [words: 841 versus 646 ms, $t(26) = 2.57$, $P = 0.016$; pseudo-words, 1092 versus 860 ms, $t(22) = 2.68$, $p = 0.013$], both groups performed close to ceiling in reading either words or pseudo-words (>92% correct).

Magnetic Resonance Imaging Protocol

All scans were acquired using a 1.5 T Signa horizon Echospeed MRI system (General Electric Medical Systems, Milwaukee, WI). High-resolution anatomical images were acquired in the axial plane using a spoiled gradient echo sequence (124 slices 1.2 mm thick, T_R = 10.3 ms, T_E = 2.1 ms, T_I = 600 ms) and 24 × 24 cm field of view (resolution of 0.937 × 0.937 × 1.2 mm). Diffusion-weighted images were acquired with echo-planar imaging in the axial plane covering the whole brain (48 slices, 2.8 mm thick, T_E = 84.4 ms, T_R 2.5 s) and 24 × 24 cm field of view (resolution 128 × 128). For each slice location, a T_2-weighted image with no diffusion sensitization, followed by five *b* values (incrementing linearly to a maximum value of 1000 s/mm^2) were obtained in six directions. In order to improve the signal-to-noise ratio, this sequence was repeated twice, providing 62 images per slice location. Before performing the tensor estimation, an unwarping algorithm was applied to the diffusion-weighted dataset to correct for distortion related to eddy currents induced by the large diffusion-sensitizing gradients (Poupon *et al.*, 2000). Thereafter, the diffusion tensor was calculated on a pixel-by-pixel basis as described previously (Pierpaoli and Basser, 1996). DTI images of one TS subject were not used because of excessive head movements during acquisition.

Voxel-based Morphometry

To characterize the local differences of cerebral tissue density between TS subjects and controls, we used a standard voxel-based morphometry approach (Ashburner and Friston, 2000; Good *et al.*, 2001). As previously described, anatomical images were processed using three different steps: creation of customized templates, normalization and smoothing (Ashburner and Friston, 2000; Good *et al.*, 2001). In the present study, we chose to investigate each hemisphere separately and excluded the cerebellum. This approach offers two advantages (Riviere *et al.*, 2002). First, it allows one to optimize the normalization on a customized template dedicated to each hemisphere and, secondly, it provides a precise analysis of medial structures without a partial volume effect of the controlateral homologue region after image smoothing. Similarly, the split of the cerebellum from each hemisphere avoids a partial volume effect of cerebellum structures on the inferior occipito-temporal region. For the first step, anatomical images of controls were normalized to Talairach space using a linear transform and the template of the Montreal Neurological Institute (MNI). After correction for standard intensity inhomogeneities of MR images, these normalized anatomical images were segmented using an automatic procedure that separates the grey and white matter from each hemisphere and from the cerebellum (Riviere *et al.*, 2002). The grey matter templates were created by averaging and then smoothing the normalized grey matter images of each hemisphere. The second step consisted in the normalization of the grey matter images in the native space onto grey matter templates. A new segmentation procedure was then applied to all the anatomical images in the native space and the resulting grey matter images were normalized to the corresponding grey matter template using a linear transform and then smoothed using a 5 mm FWHM (full width half maximum) isotropic Gaussian kernel. A similar procedure was applied to the white matter images. Lastly, we compared the smoothed grey and white matter images of each hemisphere between TS and controls on a voxel-by-voxel basis using a one-way analysis of variance (ANOVA; SPM99 software). We used a voxelwise significance threshold of 0.01 and a cluster extent threshold of $P < 0.05$ corrected for multiple comparisons across the whole brain volume. An uncorrected *P*-value of <0.005 was used for regions that were the exact controlateral homologs of any of the regions already identified, or for regions that were predicted a priori, i.e. the superior temporal sulcus and the intraparietal sulcus. In addition, similar analyses were performed with education level as a covariate in order to control for general educational differences.

Voxel based-Diffusion

Two complementary diffusion parameters were computed from the diffusion tensor: the mean diffusivity (a measure of water diffusion averaged across all directions) and the fractional anisotropy (an index of directional selectivity of water diffusion). Images of mean diffusivity and fractional anisotropy were coregistered to the anatomical images using the mutual information algorithm of SPM99. The diffusion images were then normalized to Talairach space using the linear transform calculated on the anatomical images and smoothed (FWHM: 5 mm). We compared the diffusion parameters between TS and controls on a voxel-by-voxel basis using a one-way ANOVA. We used the same thresholds as in voxel-based morphometry.

Sulcal Morphometry

To investigate further the cerebral changes identified using voxel-based analysis, we studied the sulcal morphometry of the superior temporal sulcus and of the intraparietal sulcus, two candidate regions that may underlie the cognitive impairment of TS. The superior temporal sulcus has been shown to play a crucial role in monitoring

gaze direction and in affect recognition and the intraparietal sulcus is a critical region for numerical and visuo-spatial processing. The central sulcus served as a reference sulcus for which no anomaly was expected a priori. We used an automatic sulcus extraction and identification procedure as described by Riviere *et al.* (2002). Sulci were extracted from high resolution anatomical images through a procedure that converts the anatomical images to abstract representations of the cortical folding pattern. Thereafter, an automatic recognition algorithm, using a congregation of neural networks trained on a manually labelled database, was applied for the main sulci of the cerebral cortex, except for occipital lobe sulci. As previously reported, a mean recognition rate of 76% is obtained using this method (Riviere *et al.*, 2002). Errors are mainly due to ambiguous sulci configurations. For each subject, the automatic recognition was visually verified and, if necessary, corrected. We compared the length and the maximal depth of the STS, IPS and CS between TS subjects and controls using Student's *t*-test. Values of $P < 0.05$ were considered statistically significant. Those results should be considered exploratory, given that we did not perform a Bonferoni correction for the number of comparisons performed (2 parameters × 3 sulci × 2 hemispheres = 12 comparisons total).

Results

Voxel-based Morphometry

The results of grey matter density analyses are summarized in Table 1 and are illustrated in Figure 1. Significant clusters of reduced grey matter in TS subjects compared to controls were found at symmetrical loci in anterior cingulate cortex, orbito-frontal cortex, insula, post-cental and supramarginal gyrus, and lingual gyrus. With respect to our a priori hypothesis, a decrease in the grey matter was found in the bottom of the left superior temporal sulcus and the right intraparietal sulcus. The peak difference in the grey-matter density of the right intraparietal was at Talairach coordinates (TC) –43, –30, 37 ($Z = 4{,}02$). This cluster did not survive to the correction for multiple comparisons, but this anomaly was confirmed in the sulcal morphometric analysis described below. In the opposite contrast, increase in grey-matter in TS subjects compared to controls was found symmetrically in the temporal pole, the

Table 1
Brain regions where grey matter density was significantly different between TS subjects and normal controls

Anatomical region	*P*-value cluster-level	Number of voxels (1 voxel = 1 mm^3)	*Z*-score voxel-level	Talairach coordinates (*x*, *y*, *z*)
Less grey matter in TS than in controls				
Right hemisphere				
Right anterior cingulate cortex BA 32	0.011	1413	4.93	14, 48, –3
Right lingual gyrus BA 18	<0.001	2560	4.78	10, –70, –9
Right insula BA 45	0.003	1693	4.58	30, 16, –8
Right postcentral gyrus BA 2	0.121	287	4.20	49, –25, 63
Right intraparietal sulcus BA 40	0.398	621	4.02	43, –30, 37
Right orbito-frontal cortex BA 11	0.002	1859	4.00	19, 60, –19
Right supramarginal gyrus BA 40	0.001	1961	3.94	71, –17, 26
Left hemisphere				
Left postcentral and supramarginal gyri BA 1, 2, 40	0.006	1530	4.94	–51, –23, 62
Left anterior cingulate cortex BA 32	0.121	912	4.63	–10, 51, –10
Left lingual gyrus BA 18	<0.001	2824	4.58	–7, –74, –12
Left orbito-frontal cortex BA 11	0.133	892	4.40	–20, 61, –16
Left superior temporal sulcus BA 22, 21	0.01	1431	4.09	-49, –19, –11
More grey matter in TS than in controls				
Right hemisphere				
Right temporal pole BA 38	<0.001	3624	5.20	57, 16, –11
Right postcentral and supramarginal gyri BA 1, 40	0.001	2055	4.51	50, –17, 52
Right caudate and accubens nuclei	<0.001	3954	4.35	19, –5, 24
Right orbito-frontal cortex BA 11	<0.001	2407	3.92	16, 52, –13
Right lingual gyrus BA 18	0.021	1277	3.79	3, –79, 1
Right fusiform gyrus BA 20	0.014	1375	3.75	49, –30, –34
Right orbito-frontal cortex BA 11	0.012	1402	3.54	12, 26, –31
Left hemisphere				
Left lingual gyrus BA 18	0.012	1390	4.56	–10, –82, –10
Left orbito-frontal cortex BA 11	0.003	1668	4.24	–16, –47, –16
Left temporal pole BA 38	<0.001	2452	4.03	–51, 19, –19
Left accubens nucleus	0.015	1336	3.99	–21, 18, –2
Left caudate nucleus	0.016	1324	3.90	–17, –5, 21
Left orbito-frontal cortex BA 11	0.046	1109	3.79	–8, –24, –31

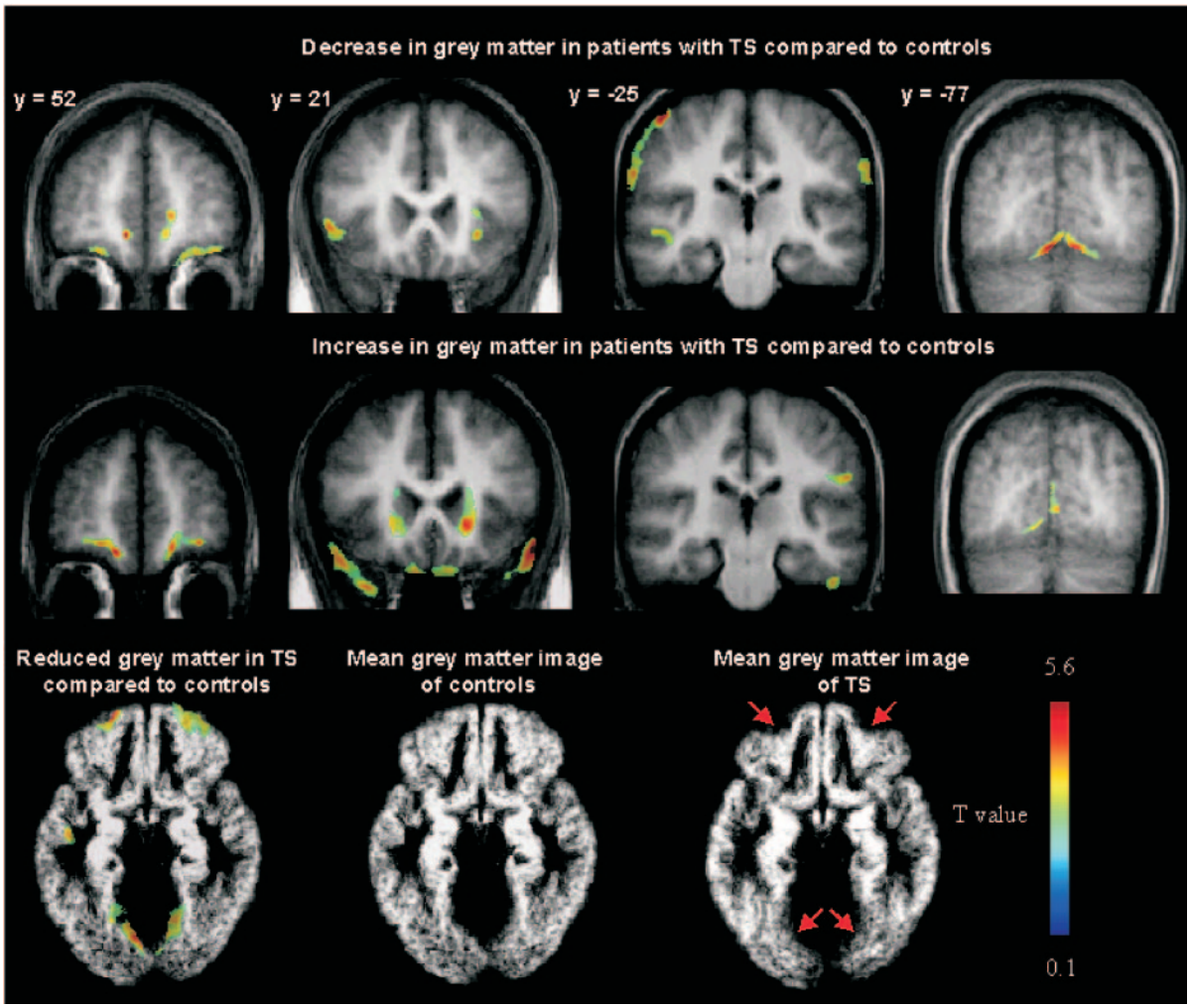

Figure 1. Brain regions showing differences in grey matter density in TS subjects compared to controls. Top row: coronal views illustrating areas with a decrease in grey matter in TS subjects compared to controls. Middle row: areas with an increase in grey matter in TS subjects. Bottom row: axial views of mean grey matter images of the 14 controls (left and middle) and the 14 TS subjects (right) showing the anatomical abnormalities in the orbito-frontal and occipito-temporal cortex of TS subjects (red arrows).

caudate nucleus and the orbito-frontal cortex and in the right lingual gyrus. The orbito-frontal and lingual clusters bordered the internal face of the orbito-frontal and lingual clusters observed in the opposite contrast. These clusters therefore seem to correspond to tissue displacement related to global atrophy of the orbito-frontal and internal occipito-temporal regions, as illustrated by the average grey matter images of controls and TS subjects (Fig. 1). An increase in grey matter was also observed in the left and right amydalae (TC –22, –3, –27, 709 voxels, Z = 3.17 and TC 28, –3, –28, 506 voxels, Z = 3.07, respectively), but these clusters did not reach statistical significance for multiple comparisons. Similar results were obtained after using the level of education as a co-variate of no interest. The results of white matter density analyses are summarized in Table 2 and showed predominant white matter differences in close proximity to the grey matter differences described above. The close match between grey and white matter results is a classical finding in voxel-based morphometry studies and may reflect an edge effect, related to a displacement of the statistical boundary between grey and white matter (Good *et al.*, 2001; Golestani *et al.*, 2002).

Voxel-based Diffusion

An increase in mean diffusivity was observed in TS subjects compared to controls in the left and right occipito-temporal region, the left lingual gyrus, the right fusiform gyrus and the left and right cerebellum (Table 3 and Fig. 2). No significant cluster was observed in the opposite contrast for regions of decrease in mean diffusivity in TS group compared to controls.

Increase in anisotropy in TS group compared to controls was found bilaterally in depth of the superior temporal sulcus, in the right semi-ovale centrum and in the right external capsule (Table 3 and Fig. 3). Two symmetrical clusters of decreased anisotropy were observed in the temporal white matter in regions with increased mean diffusivity (Table 3 and Fig. 2). However, no clusters of decreased anisotropy survived at corrected P-value.

Analyses of Fiber Orientation within the Temporal Lobe

From DTI, the main diffusion direction within each voxel can be used to infer fiber orientation in the region of abnormal

Table 2
Brain regions where white matter density was significantly different between TS subjects and normal controls

Anatomical region	*P*-value cluster-level	Number of voxels (1 voxel = 1 mm^3	*Z*-score voxel-level	Talairach coordinates (*x*, *y*, *z*)
Less white matter in TS than in controls				
Right hemisphere				
Adjacent to the head of right caudate nucleus	0.066	1127	4.43	19, 19, –8
Adjacent to right post central sulcus	0.042	1237	4.27	50, –19, 49
Adjacent to the body of right caudate nucleus	0.014	416	4.19	26, –7, 27
Adjacent to right supramarginal gyrus	0.024	1376	3.70	58, –26, –25
Left hemisphere				
Adjacent to the left superior temporal sulcus	0.018	1449	4.87	–45, –17, –6
Adjacent to left lingual gyrus	0.001	2222	4.85	–9, –82, –9
Adjacent to the head of left caudate nucleus	0.001	642	4.28	–21, 17, –2
Left occipito-parietal region	0.008	1658	4.61	–20, 86, 24
Adjacent to left body of right caudate nucleus	0.022	1390	3.26	–18, –5, –19
More white matter in TS than in controls				
Right hemisphere				
Right external capsule	0.002	2042	5.50	31, 17, –7
Adjacent to right intraparietal sulcus	0.035	1280	3.62	42, –30, 37
Body of corpus callosum	0.038	332	3.55	11, 6, 24
Adjacent to right anterior cingulate cortex	0.319	748	3.81	14, 50, 0
Left hemisphere				
Adjacent to left anterior cingulate cortex	0.151	936	4.97	–8, 62, 3
Adjacent to superior temporal gyrus	0.014	505	4.33	–49, –19, –11
Body of corpus callosum	0.044	1224	3.22	–11, 2, 26

Table 3
Brain regions where mean diffusivity and fractional anisotropy were significantly different between TS subjects and normal controls

Anatomical region	*P*-value cluster-level	Number of voxels (1 voxel = 9 mm^3	*Z*-score voxel-level	Talairach coordinates (*x*, *y*, *z*)
Increase in mean diffusivity in TS relative to controls				
Right fusiform gyrus BA 19	0.006	129	4.44	42, –66, –9
Left and right cerebellum, left lingulal gyrus BA 18	<0.001	406	4.23	–9, –93, –36
Right temporo-occipital region	0.032	98	3.62	39, –42, 15
Left temporo-occipital region	0.001	167	3.45	–48, –15, –27
			3.36	–36, –48, 3
Left cerebellum, fourth ventricle	0.003	145	3.33	–6, –66, –51
Decrease in mean diffusivity in TS relative to controls: none				
Increase in fractional anisotropy in TS relative to controls				
Right semi-ovale centrum	0.019	109	4.57	30, –3, 33
Right superior temporal sulcus, right middle temporal gyrus	0.573	47	4.43	48, 0, –24
Left superior temporal sulcus, left middle temporal gyrus, left temporo-occipito-parietal region	<0.001	199	4.25	–51, –18, –12
Right external capsule	0.047	92	3.82	39, 3, –15
Decrease in fractional anisotropy in TS relative to controls				
Right inferior occipito-temporal white matter	0.778	26	3.87	39, –45, –6
Left inferior occipito-temporal white matter	0.188	49	3.46	–36, –45, 0

white matter in TS. In Figure 2, fiber orientation in one control is represented using a color code for the orientation of the main temporal fiber tracts. The orientation of fibers within the two temporal clusters of increased mean diffusivity has a clear antero-posterior direction (shown in green in Fig. 2), suggesting microstructural alterations of sagittally oriented

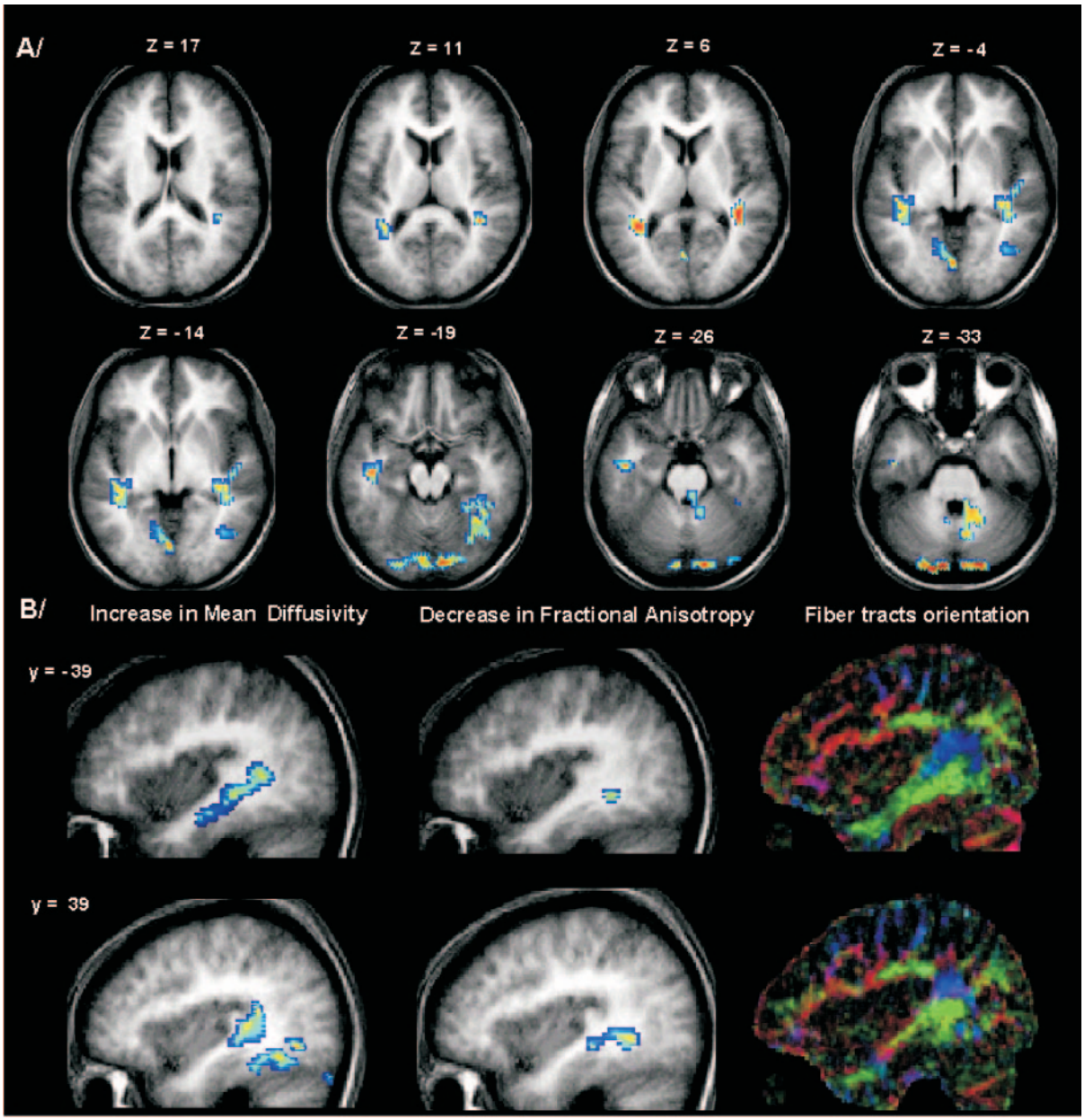

Figure 2. Brain regions with an increase in mean diffusivity in TS subjects compared to controls (*A*). Note the bilateral and symmetric diffusion changes in the temporal white matter in areas where no macroscopical abnormality was observed on anatomical images. Sagittal views showing temporal clusters with diffusion changes in TS group and analyses of fiber tracts orientation in one control at the same level (*B*). Right: in this RGB encoded plot, red voxels correspond to left-right direction of diffusion, blue voxels to a superior–inferior orientation and green voxels to an antero-posterior orientation. The increase in mean diffusivity and the decrease in anisotropy affect electively antero-posterior pathways, suggesting a disconnection between anterior and posterior regions within the temporal lobe.

white matter tracts. The other clusters of abnormal diffusion do not have a clear preferential orientation.

Sulcal Morphometry

Sulcal morphometry was investigated for the superior temporal sulcus and the intraparietal sulcus, two sulci for which we have a priori hypotheses based on the cognitive profile of TS. The central sulcus was used as a reference sulcus for which no impairment was expected (Fig. 4). For the central sulcus, both length and maximal depth did not differ between TS subjects and controls. However, the maximal depth of the left and right superior temporal sulci was significantly smaller in TS subjects than in controls (mean ± standard error: left side, TS = 25.2 ± 0.8 mm, controls = 27.7 ± 0.7, $P = 0.03$; right side, TS = 28.4 ± 0.4, controls = 31.5 ± 0.8, $P = 0.003$). Sulcal length was unaffected. For the right intraparietal sulcus, we observed a significant decrease in maximal depth (TS = 28.1 ± 0.83, controls = 30.7 ± 0.6, $P = 0.005$). There was also a trend for length reduction (TS = 516 ± 34, controls = 606 ± 26, $P = 0.057$). No difference in either length and depth was observed for the left intraparietal sulcus.

Discussion

Our study provides converging evidence of regionally specific structural changes in TS at both macroscopical and microscopical levels using two independent neuroimaging methods,

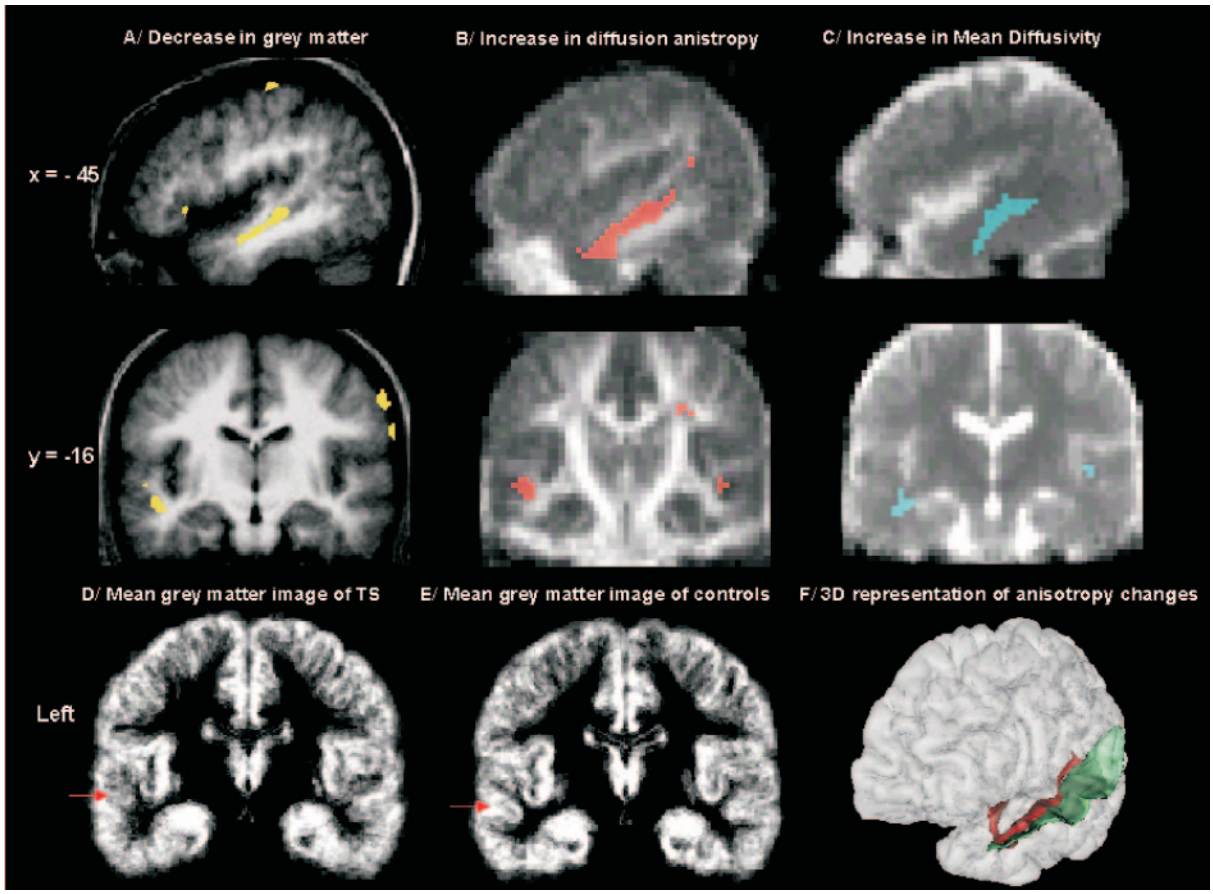

Figure 3. Converging results showing the abnormalities of the left superior temporal sulcus in TS subjects. Abnormalities in a similar region of the left superior temporal sulcus are found on both anatomical images (*A*) (yellow clusters)and on fractional anisotropy images (*B*) (red clusters). Increase in mean diffusivity (*C*) (blue clusters) in the temporal white matter of TS subjects suggests microstrutucral changes of projections pathways. The differences in the left superior temporal sulcus are clearly illustrated by the visual examination of the mean image of grey matter of 14 TS subjects (*D*) compared to those of the mean image of the 14 controls (*E*) (red arrows). Fractional anisotropy changes (*F*) (red) are observed along the superior temporal sulcus (green) at the grey–white matter interface.

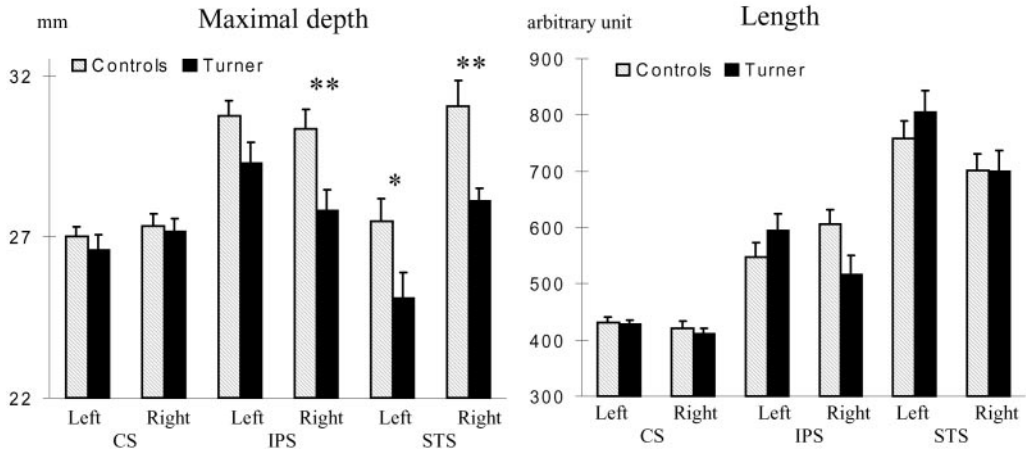

Figure 4. Histograms of length and maximal depth of the central sulcus (CS), the superior temporal sulcus (STS) and the intraparietal sulcus (IPS). A significant decrease in maximal depth is found in the left and right superior temporal sulci and in the right intraparietal sulcus in TS subjects compared to controls (*$P < 0.05$, **$P < 0.005$). A trend towards a decrease in length of the right intraparietal is also observed.

high-resolution anatomical T_1-weighted imaging and diffusion tensor imaging. The voxel-based analysis of anatomical images provided evidence for macroscopical changes in several cortical regions: bilateral orbito-frontal and anterior cingulate regions, temporal poles and lingual gyri, the left superior temporal sulcus and the right intraparietal sulcus. Further below, we will consider the extent to which those abnormalities can be related to TS subjects' deficits in two main domains, social

abilities and visuo-spatial/numerical processing. The analysis of diffusion anisotropy images indicated the presence of white matter in TS subjects at coordinates that correspond to the grey matter located at bottom of the left superior temporal sulcus in controls, confirming a displacement of the grey–white matter interface in this sulcus (Fig. 3). A smaller but symmetrical anomaly was present in the right superior temporal sulcus. Diffusion images also revealed a symmetrical and bilateral increase in mean diffusivity and decrease in anisotropy in the temporal white matter that seemed macroscopically normal on anatomical images (Fig. 2). The analysis of fibers orientation showed that areas with diffusion changes contain fiber tracts with a posterior to anterior orientation, suggesting microstructural changes of sagittally oriented pathways in the temporal lobes. This finding is consistent with anatomical studies showing that, within these temporo-occipital regions, axons are running oriented sagittally in the inferior longitudinal fasciculus (Dejerine, 1895; Crosby *et al.*, 1962). This fasciculus contains mainly long association fibers connecting the temporal pole to the occipital pole, but also carries some shorter cortico-cortical fibers (Gloor, 1997). These microstructural anomalies plausibly alter the connections between anterior and posterior regions of the temporal lobes. This appears particularly relevant in the context of bilateral macroscopical anomalies of grey matter distribution in the lingual gyrus, in the superior temporal regions and temporal poles. Finally, analyses of sulcal morphometry confirmed the anomalies found in the left and right superior temporal sulcus and in the right intraparietal sulcus and further clarified voxel-based analyses by showing an abnormal depth of these sulci.

Methodological Issues

Before proposing a functional interpretation of our results, it is important to keep in mind the limitations, but also the complementarity, of our methods. The first limitation of this study concerns its design and is mainly due to the low prevalence and the difference in education level of TS subjects. We acknowledge that, although similar to other studies in TS or utilizing DTI, the number of subjects included in this study is rather small and thus was not designed to represent an unbiased sample of TS. The inclusion of mosaic genotypes is also a potential confound, but the presence of soma normal cell lines in mosaic genotypes would argue against the possibility of finding group differences. Moreover, the identification of mosaicism depends directly on the method of ascertainment and tissue-specific karyotyping can give divergent results (Saenger, 1996; Ranke and Saenger, 2001). Some authors have also argued that mosaicism with a normal cell line in fetal membranes may be necessary for adequate placental function and fetal survival (Saenger, 1996; Ranke and Saenger, 2001). The expected difference in education level between the two groups raises the issue of the contribution to our results of the general cognitive functioning of the TS subjects. However, the anatomical differences that we found in TS do not coincide with regions that were reported to correlate with IQ (Duncan *et al.*, 2000; Thompson *et al.*, 2002) and the use of education level as a covariate did not influence our results.

A second limitation of this study concerns the sensitivity of MR based techniques. Voxel-based morphometry of T_1 images detects macroscopic changes in the distribution of grey matter. Such changes are generally interpreted as reflecting an abnormal organization of brain tissue. However, they may potentially be due to a local deformation of brain shape secondary to more global changes in skeletal anatomy, which may have little or no impact on brain function. This could be important given that the physical phenotype of TS patients includes skeletal anomalies that may also influence the skull. Some effort was made to control for such global factors by first normalizing the global brain shape onto a common template prior to statistical analysis. Conversely, anomalies in internal regions such as the anterior cingulate, superior temporal and intraparietal sulcus are unlikely to be modulated by major changes in brain shape and are more likely to reflect genuine structural disorganization, especially when they are confirmed by direct measurement of sulcal depth. There are also no clear predictions on the direction of the expected grey matter changes in developmental disorders and, similarly to previous voxel-based morphometry studies in developmental disorders such as autism or fetal alcohol syndrome, our results revealed that the grey matter density in TS can decrease or increase in different brain regions. The interpretation of such results is crucially dependant on cross-validation using complementary methods such as diffusion tensor imaging and sulcal morphometry. Relative to the information provided by anatomical images, diffusion images, which reflect the Brownian motion of water molecules at a scale of ~10 μm, provide access to independent information on the microstructure of brain tissue. Once the images of patients and controls are correctly aligned, so that measurement is effected within regions of white matter that appear normal on anatomical images, diffusion reflects the fine-grained organization of fiber tracts. In the present work, increases in mean diffusivity were found in the white matter that appeared normal on anatomical images, particularly in the white matter underneath the temporal lobes, suggesting a microstructural disorganization of a major antero-posterior fiber tract. Few changes in anisotropy were observed in these regions. Significant anisotropy changes observed elsewhere in the brain seemed to reflect displacement of the boundary between grey and white matter in patients compared to controls.

Deficits in Social Cognition

Numerous psychological studies have reported psychosocial difficulties in TS. Compared to controls, subjects with TS have fewer friends, engage in fewer social activity and show affective immaturity and attentional deficits (McCauley *et al.*, 1986a,b, 1995; Mazzocco *et al.*, 1998; Ross *et al.*, 2000). These social difficulties might be dismissed as secondary to the daily life difficulties associated with TS phenotype (e.g small size), but they might also indicate a specific deficit in social cognition. Autistic features have been described in TS subjects and a 500-fold increased risk of autism is associated with TS (Skuse *et al.*, 1997; Creswell and Skuse, 2000). As in autistic children, TS patients showed deficits both in face recognition and in affect recognition on facial expressions (Elgar *et al.*, 2002; Lawrence *et al.*, 2003). Converging evidence suggests that social perception from visual cues involves specific brain regions and, in particular, the superior temporal sulcus in both hemispheres (Allison *et al.*, 2000; Frith, 2001). Neuroimaging studies using PET and fMRI have pinpointed activations of the left and right superior temporal sulci during the detection of eye gaze and the perception of biological motion such as lip-reading (Allison *et al.*, 2000). In monkeys, single cell recordings revealed neurons in the superior temporal sulcus that respond

according to gaze direction. Furthermore, lesions of the superior temporal sulcus in monkeys lead to impaired judgements of gaze directions (Perrett *et al.*, 1985). Taken together, such data suggest that the bilateral superior temporal sulcus anomalies that we have observed in TS subjects constitute the cerebral bases of deficits in social perception from visual cues. Besides the crucial role of superior temporal sulcus in the social perception, single cells recordings in monkeys and neuroimaging studies in humans have also suggested that social cognition involves an extended bilateral network including the amygdala, temporal pole, orbito-frontal cortex and anterior cingulate (Happe *et al.*, 1996; Baron-Cohen *et al.*, 1999; Allison *et al.*, 2000; Frith, 2001). It is remarkable that all of these regions were found anomalous in our anatomical analyses and this fits particularly well with the hypothesis of an impairment of 'the social brain' in TS. Moreover, the diffusion changes within the temporal lobes suggest microstructural changes of the long distance antero-posterior temporal projections, which may plausibly disconnect the different components of this network and, in particular, the temporal pole and the superior temporal region. Lastly, this conclusion entails an implication of X-linked genes in the development of the cerebral networks for social cognition. This fits with the greater vulnerability of males to developmental disorders of language and social cognition, such as autism (Creswell and Skuse, 2000) and with a previous report suggesting a role of an imprinted X-linked locus in social cognition (Skuse *et al.*, 1997). A recent MRI study in TS using regional measurements did not find any influence of genomic imprinting on cerebral lobes volumes (Brown *et al.*, 2002). However, the present fine-grained methods may be better adapted to reveal such subtle differences. In the present study, we did not ascertain whether the remaining X chromosome was maternal or paternal. Future studies focusing on the brain regions found abnormal in this study are needed to investigate the possible influence of genomic imprinting on the development of cerebral networks involved in social cognition.

Deficits in Spatial–Numerical Processing

Visuo-spatial deficits in TS include difficulties in judgement of line orientation, mental rotation in space and right–left disorientation in extrapersonal space (Alexander and Money, 1966; Rovet and Netley, 1980; Pennington *et al.*, 1985; Temple and Carney, 1995; Ross *et al.*, 2002). TS subjects also experience difficulties in mathematics, particularly in arithmetical tasks such as subtraction, operations with large numbers, subitizing and cognitive estimation (Pennington *et al.*, 1985; Rovet *et al.*, 1994; Mazzocco, 1998; Temple and Marriot, 1998; Butterworth *et al.*, 1999; Ross *et al.*, 2002; Bruandet *et al.*, 2004). These deficits in TS are consistent across a wide range of ages and are not reversible with estrogen substitution (Ross *et al.*, 2002). In particular, several tests confirmed that the TS subjects included in this study were impaired in arithmetic (Molko *et al.*, 2003). For instance, they performed significantly worse than controls on Warrington's graded arithmetic test, a graded difficulty test of arithmetic computations. Neuropsychological and functional neuroimaging studies in normal subjects and in patients with cerebral lesions have provided compelling evidence for the crucial role of the intraparietal sulcus in visuo-spatial and numerical processing (Cohen and Dehaene, 1994; Dehaene and Cohen, 1997; Dehaene *et al.*, 1998; Lee, 2000; Stanescu-Cosson *et al.*, 2000). Functional imaging in normal subjects has revealed that numerical quantity manipulation relies on a reproducible cerebral network that systematically involves the left and right intraparietal sulci, with increasing activation as the task puts greater emphasis on quantity processing (Dehaene *et al.*, 1999; Pinel *et al.*, 2001). Anatomical MRI studies in developmental dyscalculia have shown a clear impairment of the left parietal cortex, (Levy *et al.*, 1999; Isaacs *et al.*, 2001). In particular, using voxel-based morphometry, a decrease in the grey matter density has been found in the left intraparietal sulcus (TC: −39, −39, 45) in premature children with dyscalculia (Isaacs *et al.*, 2001). In the present study, a decrease in grey matter subjects was found at a symmetrical location in the right intraparietal sulcus of TS subjects (TC: 43, −30, 37). Morphometric analysis of the right intraparietal sulcus revealed that this sulcus was shallower and tended to be shorter in TS. The finding of a morphological difference in the right intraparietal sulcus is consistent with the results of our fMRI study during calculation tasks in the same TS subjects. We found that, while TS activated the classical parieto-frontal network during calculation tasks, a decreased activation in the right intraparietal sulcus was observed when the tasks put greater emphasis on exact calculation with large numbers (Molko *et al.*, 2003). This decreased activation in the right intraparietal sulcus during calculation tasks is closely located to the region found abnormal using voxel-based morphometry (TC: 48, −36, 48). Our results suggest that reduced grey matter in the right intraparietal sulcus may be responsible for the visuo-spatial and number processing deficits in TS. More broadly, this result and the previous report in children with developmental dyscalculia associated with prematurity suggest that the intraparietal sulcus may play a crucial role in developmental dyscalculia, although the possibility of a distinct role of the left and right intraparietal sulci remains to be clarified.

Executive Function Deficits

Reduced performance on tests classically associated with frontal lobe function such as the *n*-back task, the tower of Hanoi task, the Wisconsin card sorting test and verbal fluency has been repeatedly reported in TS (Waber, 1979; Bender *et al.*, 1993; Temple *et al.*, 1996; Romans *et al.*, 1998; Haberecht *et al.*, 2001). Our results do not provide evidence for anatomical changes in the lateral prefrontal cortex. Although we cannot exclude that a subtle deficit might be identified with higher resolution images, our result is consistent with previous volumetric MRI studies (Murphy *et al.*, 1993; Reiss *et al.*, 1993, 1995; Brown *et al.*, 2002). However, the anatomical changes found in the right parietal lobe and in the left and right cingulate cortex may be plausibly related to the executive impairment in TS and may cause functional rather than anatomical changes in prefrontal regions. Two recent fMRI studies in TS during frontal tasks have shown bilateral abnormal prefrontal activations. Decreased activations have been found bilaterally in the dorso-lateral prefrontal cortex and also in the supramarginal gyrus during *n*-back tasks (Haberecht *et al.*, 2001) and increased activations in the superior and middle frontal gyri have been also reported during a go–no-go task (Tamm *et al.*, 2003). Finally, one should stress that the neuropsychological tasks used in TS studies such as the tower of Hanoi task, the Wisconsin card sorting test, or verbal fluency, do not isolate an individual cognitive process and do not target a precise anatomical region. A more detailed analysis of executive dysfunction in TS is needed to disentangle the relative contri-

butions of spatial and verbal working memory, attention and inhibition.

In conclusion, our MRI study used two independent MRI techniques to provide converging evidence of regionally specific structural changes in TS. The multifocal and bilateral cerebral abnormalities found in TS are highly consistent with the hallmark symptoms associated with TS. In particular, our results showed bilateral macroscopic anomalies in the main components of a distributed network implicated in social cognition and microstructural alterations in the putative temporal connections of this network. A more focal anomaly was also found in the right intraparietal sulcus, which has been implicated in visuo-spatial and numerical processing. The observation that a genetic X-linked disease can impair social and spatial–numerical cognition strengthens the hypothesis that those functions are laid down by genetic and neurobiological systems in the course of both phylogenetic evolution and child development (Brothers, 1990; Dehaene *et al.*, 1998; Allison *et al.*, 2000). Although it is currently hard to separate direct genetic effects on brain development from indirect effects of hormonal depletion in TS, the correlation of genetic anomalies with functional and anatomical imaging methods provides a powerful method to narrow down the search for genes involved in brain cognition and in cognitive development (Watkins *et al.*, 2002).

Notes

We are indebted to the members of the French Turner syndrome association (AGAT association) for their continued cooperation with our research programme. We also wish to thank Professor Jean-Claude Carel from Saint-Vincent-de-Paul hospital and INSERM U342 for his help in the recruitment. This work was supported by INSERM, CEA and a centennial fellowship of the McDonell Foundation to S.D.

Address correspondence to Nicolas Molko, INSERM U 562, Service Hospitalier Frédéric Joliot, CEA/DSV, 4 Place du general Leclerc 91401 Orsay cedex, France. Email: molko@wanadoo.fr.

References

Alexander D, Money J (1966) Turner syndrome and Gerstmann's syndrome: neuropsychological comparison. Neuropsychologia 4:265–273.

Allison T, Puce A, McCarthy G (2000) Social perception from visual cues: role of the STS region. Trends Cogn Sci 4:267–278.

Ashburner J, Friston KJ (2000) Voxel-based morphometry — the methods. Neuroimage 11:805–821.

Baron-Cohen S, Ring HA, Wheelwright S, Bullmore ET, Brammer MJ, Simmons A, Williams SC (1999) Social intelligence in the normal and autistic brain: an fMRI study. Eur J Neurosci 11:1891–1898.

Bender BG, Linden MG, Robinson A (1993) Neuropsychological impairment in 42 adolescents with sex chromosome abnormalities. Am J Med Genet 48:169–173.

Brothers L (1990) The social brain: a project for integrating primate behaviour and neurophysiology in a new domain. Concepts Neurosci 1:27–51.

Brown WE, Kesler SR, Eliez S, Warsofsky IS, Haberecht M, Patwardhan A, *et al.* (2002)Brain development in Turner syndrome: a magnetic resonance imaging study. Psychiatry Res 116:187–196.

Bruandet M, Molko N, Cohen L, Dehaene S (2004) A cognitive characterisation of dyscalculia in Turner syndrome. Neuropsychologia 42:288–298.

Butterworth B, Grana A, Piazza M, Price CJ, Skuse D (1999) Language and the origins of number skills. Brain Lang 96:486–488.

Clark C, Klonoff H, Hayden M (1990) Regional cerebral glucose metabolism in Turner syndrome. Can J Neurol Sci 17:140–144.

Cohen L, Dehaene S (1994) Amnesia for arithmetic facts: a single case study. Brain Lang 47:214–232.

Conturo TE, Lori NF, Cull TS, Akbudak E, Snyder AZ, Shimony JS, *et al.* (1999) Tracking neuronal fiber pathways in the living human brain. Proc Natl Acad Sci USA 96:10422–10427.

Creswell C, Skuse D (2000) Autism in association with Turner syndrome: implications for male vulnerability to pervasive developmental disorders. Neurocase 5:511–518.

Crosby EC, Humphrey T, Lauer EW (1962) Anatomy of the nervous system. New York: Macmillian.

Dehaene S, Cohen L (1997) Cerebral pathways for calculation: double dissociation between rote verbal and quantitative knowledge of arithmetic. Cortex 33:219–250.

Dehaene S, Dehaene-Lambertz G, Cohen L (1998) Abstract representations of numbers in the animal and human brain. Trends Neurosci 21:355–361.

Dehaene S, Spelke E, Pinel P, Stanescu R, Tsivkin S (1999) Sources of mathematical thinking: behavioral and brain-imaging evidence. Science 284:970–974.

Dejerine J (1895) Anatomie des centres nerveux, Vol 1. Paris: Rueff.

Duncan J, Seitz RJ, Kolodny J, Bor D, Herzog H, Ahmed A, *et al.* (2000) A neural basis for general intelligence. Science 289:457–460.

Elgar K, Campbell R, Skuse D (2002) Are you looking at me? Accuracy in processing line-of-sight in Turner syndrome. Proc R Soc Lond B Biol Sci 269:2415–2422.

Frith U (2001) Mind blindness and the brain in autism. Neuron 32:969–979.

Gloor P (1997) The temporal lobe and the limbic system. New York: Oxford University Press.

Golestani N, Paus T, Zatorre RJ (2002) Anatomical correlates of learning novel speech sounds. Neuron 35:997–1010.

Good CD, Johnsrude IS, Ashburner J, Henson RN, Friston KJ, Frackowiak RS (2001) A voxel-based morphometric study of ageing in 465 normal adult human brains. Neuroimage 14:21–36.

Good CD, Lawrence K, Thomas NC, Price C, Ashburner J, Friston K, *et al.* (2003) Dosage-sensitive X-linked locus influences the development of amygdala and orbito-frontal cortex, and fear recognition in humans. Brain 126:1–16.

Haberecht MF, Menon V, Warsofsky IS, White CD, Dyer-Friedman J, Glover GH, *et al.* (2001) Functional neuroanatomy of visuo-spatial working memory in Turner syndrome. Hum Brain Mapp 14:96–107.

Happe F, Ehlers S, Fletcher P, Frith U, Johansson M, Gillberg C, *et al.* (1996) 'Theory of mind' in the brain. Evidence from a PET scan study of Asperger syndrome. Neuroreport 8:197–201.

Isaacs EB, Edmonds CJ, Lucas A, Gadian DG (2001) Calculation difficulties in children of very low birthweight: a neural correlate. Brain 124:1701–1707.

Jackson, M and Warrington, EK (1986) Arithmetic skills in patients with unilateral cerebral lesions. Cortex 22:611–620.

Klingberg T, Hedehus M, Temple E, Salz T, Gabrieli JD, Moseley ME, *et al.* (2000) Microstructure of temporo-parietal white matter as a basis for reading ability: evidence from diffusion tensor magnetic resonance imaging. Neuron 25:493–500.

Lawrence K, Kuntsi J, Coleman M, Campbell R, Skuse D (2003) Face and emotion recognition deficits in Turner syndrome: a possible role for X-linked genes in amygdala development. Neuropsychology 17:39–49.

Le Bihan D, Mangin JF, Poupon C, Clark CA, Pappata S, Molko N, *et al.* (2001) Diffusion tensor imaging: concepts and applications. J Magn Resonon Imaging 13:534–546.

Lee KM (2000) Cortical areas differentially involved in multiplication and subtraction: a functional magnetic resonance imaging study and correlation with a case of selective acalculia. Ann Neurol 48:657–661.

Levy LM, Reis IL, Grafman J (1999) Metabolic abnormalities detected by 1H-MRS in dyscalculia and dysgraphia. Neurology 53:639–641.

McCauley E, Ito J, Kay T (1986a) Psychosocial functioning in girls with Turner's syndrome and short stature: social skills, behavior problems, and self-concept. J Am Acad Child Psychiatry 25:105–112.

McCauley E, Sybert VP, Ehrhardt AA (1986b) Psychosocial adjustment of adult women with Turner syndrome. Clin Genet 29:284–290.

McCauley E, Ross JL, Kushner H, Cutler G Jr (1995) Self-esteem and behavior in girls with Turner syndrome. J Dev Behav Pediatr 16:82–88.

Maguire EA, Gadian DG, Johnsrude IS, Good CD, Ashburner J, Frackowiak RS, *et al.* (2000) Navigation-related structural change in the hippocampi of taxi drivers. Proc Natl Acad Sci USA 97:4398–4403.

Mazzocco MM (1998) A process approach to describing mathematics difficulties in girls with Turner syndrome. Pediatrics 102:492–496.

Mazzocco MM, Baumgardner T, Freund LS, Reiss AL (1998) Social functioning among girls with fragile X or Turner syndrome and their sisters. J Autism Dev Disord 28:509–517.

Molko N, Cachia A, Riviere D, Mangin JF, Bruandet M, Le Bihan D, Cohen L, Dehaene S (2003) Functional and structural alterations of the intraparietal sulcus in a developmental dyscalculia. Neuron 40: 847–858.

Murphy DG, DeCarli C, Daly E, Haxby JV, Allen G, White BJ, *et al.* (1993) X-chromosome effects on female brain: a magnetic resonance imaging study of Turner's syndrome. Lancet 342:1197–1200.

Murphy DG, Mentis MJ, Pietrini P, Grady C, Daly E, Haxby JV, *et al.* (1997) A PET study of Turner's syndrome: effects of sex steroids and the X chromosome on brain. Biol Psychiatry 41:285–298.

Pennington BF, Heaton RK, Karzmark P, Pendleton MG, Lehman R, Shucard DW (1985) The neuropsychological phenotype in Turner syndrome. Cortex 21:391–404.

Perrett DI, Smith PA, Potter DD, Mistlin AJ, Head AS, Milner AD, *et al.* (1985) Visual cells in the temporal cortex sensitive to face view and gaze direction. Proc R Soc Lond B Biol Sci 223:293–317.

Pierpaoli, C and Basser, PJ (1996) Toward a quantitative assessment of diffusion anisotropy. Magn Reson Med 36:893–906.

Pierpaoli C, Jezzard P, Basser PJ, Barnett A, Di Chiro G (1996) Diffusion tensor MR imaging of the human brain. Radiology 201:637–648.

Pinel P, Dehaene S, Riviere D, LeBihan D (2001) Modulation of parietal activation by semantic distance in a number comparison task. Neuroimage 14:1013–1026.

Poupon C, Clark CA, Frouin V, Regis J, Bloch I, Le Bihan D, *et al.* (2000) Regularization of diffusion-based direction maps for the tracking of brain white matter fascicles. Neuroimage 12:184–195.

Ranke MB, Saenger P (2001) Turner's syndrome. Lancet 358:309–314.

Reiss AL, Freund L, Plotnick L, Baumgardner T, Green K, Sozer AC, *et al.* (1993) The effects of X monosomy on brain development: monozygotic twins discordant for Turner's syndrome. Ann Neurol 34:95–107.

Reiss AL, Mazzocco MM, Greenlaw R, Freund LS, Ross JL (1995) Neurodevelopmental effects of X monosomy: a volumetric imaging study. Ann Neurol 38:731–738.

Riviere D, Mangin JF, Papadopoulos-Orfanos D, Martinez J, Frouin V, Regis J (2002) Automatic recognition of cortical sulci of the human brain using a congregation of neural networks. Med Image Anal 6:77–92.

Romans SM, Stefanatos G, Roeltgen DP, Kushner H, Ross JL (1998) Transition to young adulthood in Ullrich–Turner syndrome: neurodevelopmental changes. Am J Med Genet 79:140–147.

Rose SE, Chen F, Chalk JB, Zelaya FO, Strugnell WE, Benson M, *et al.* (2000) Loss of connectivity in Alzheimer's disease: an evaluation of white matter tract integrity with colour coded MR diffusion tensor imaging. J Neurol Neurosurg Psychiatryry 69:528–530.

Ross J, Zinn A, McCauley E (2000) Neurodevelopmental and psychosocial aspects of Turner syndrome. Ment Retard Dev Disabil Res Rev 6:135–141.

Ross JL, Stefanatos GA, Kushner H, Zinn A, Bondy C, Roeltgen D (2002) Persistent cognitive deficits in adult women with Turner syndrome. Neurology 58:218–225.

Rovet J, Netley C (1980) The mental rotation task performance of Turner syndrome subjects. Behav Genet 10:437–443.

Rovet J, Szekely C, Hockenberry MN (1994) Specific arithmetic calculation deficits in children with Turner syndrome. J Clin Exp Neuropsychol 16:820–839.

Saenger P (1996) Turner's syndrome. N Engl J Med 335:1749–1754.

Skuse DH, James RS, Bishop DV, Coppin B, Dalton P, Aamodt-Leeper G, *et al.* (1997) Evidence from Turner's syndrome of an imprinted X-linked locus affecting cognitive function. Nature 387:705–708.

Sluming V, Barrick T, Howard M, Cezayirli E, Mayes A, Roberts N (2002) Voxel-based morphometry reveals increased gray matter density in Broca's area in male symphony orchestra musicians. Neuroimage 17:1613–1622.

Sowell ER, Thompson PM, Mattson SN, Tessner KD, Jernigan TL, Riley EP, *et al.* (2001) Voxel-based morphometric analyses of the brain in children and adolescents prenatally exposed to alcohol. Neuroreport 12:515–523.

Stanescu-Cosson R, Pinel P, van De Moortele PF, Le Bihan D, Cohen L, Dehaene S (2000) Understanding dissociations in dyscalculia: a brain imaging study of the impact of number size on the cerebral networks for exact and approximate calculation. Brain 123:2240–2255.

Tamm L, Menon V, Reiss AL (2003) Abnormal prefrontal cortex function during response inhibition in turner syndrome: functional magnetic resonance imaging evidence. Biol Psychiatry 53:107–111.

Temple CM, Carney RA (1995) Patterns of spatial functioning in Turner's syndrome. Cortex 31:109–118.

Temple CM, Carney R (1996) Reading skills in children with Turner's syndrome: an analysis of hyperplexia. Cortex 32:335–345.

Temple CM, Marriot AJ (1998) Arithmetical ability and disability in Turner 's syndrome: a cognitive neuropsychological analysis. Dev Neuropsychol 14:47–67.

Temple CM, Sherwood S (2002) Representation and retrieval of arithmetical facts: developmental difficulties. Q J Exp Psychol A 55:733–752.

Temple CM, Carney R, Mullarkey S (1996) Frontal lobe function and executive skills in children with Turner's syndrome. Dev Neuropsychol 12:343–363.

Thompson PM, Cannon TD, Narr KL, Van Erp T, Poutanen VP, Huttunen M, *et al.* (2002) Genetic influences on brain structure. Nat Neurosci 4:1153–1154.

Turner H (1938) A syndrome of infantilism, congenital webbed neck and cubitus valgus. Endocrinology 28:566–574.

Waber DP (1979) Neuropsychological aspects of Turner's syndrome. Dev Med Child Neurol 21:58–70.

Watkins KE, Vargha-Khadem F, Ashburner J, Passingham RE, Connelly A, Friston KJ, *et al.* (2002) MRI analysis of an inherited speech and language disorder: structural brain abnormalities. Brain 125:465–478.

Wolkin A, Choi SJ, Szilagyi S, Sanfilipo M, Rotrosen JP, Lim KO (2003) Inferior frontal white matter anisotropy and negative symptoms of schizophrenia: a diffusion tensor imaging study. Am J Psychiatry 160:572–574.